Crucial role of sustainable liquid junction potential for solar-to-carbon monoxide conversion by photovoltaic photoelectrochemical system

Yoshitsune Sugano,*[a] Akihiko Ono,[a] Ryota Kitagawa,[a] Jun Tamura,[a] Masakazu Yamagiwa,[a] Yuki Kudo,[a] Eishi Tsutsumi[a] and Satoshi Mikoshiba[a]

[a] *Corporate Research & Development Center, Toshiba Corporation, Kawasaki 212-8582, Japan*

E-mail: yoshitsune.sugano@toshiba.co.jp

Electronic Supplementary Information (ESI†)

Detailed explanation of the theoretical estimation of solar-to-CO conversion efficiency

Theoretical estimation of electrode properties: Obtaining closer estimated results of solar-to-CO conversion efficiency requires accurate understanding of the overpotentials. Based on the Arrhenius equation, the reaction current density includes the mass transfer process and the charge transfer process according to the following equation:

$$J = J_0 \cdot \left[\left(\frac{C_R^s}{C_R^{eq}} \right) \cdot \exp\left(\frac{\alpha_a n F \Delta V_a}{RT} \right) - \left(\frac{C_O^s}{C_O^{eq}} \right) \cdot \exp\left(\frac{-\alpha_c n F \Delta V_c}{RT} \right) \right]$$

J, J_0, C^s, C^{eq}, α, n, F, ΔV, R, and T are respectively current density, exchange current density, electrode surface concentration, equilibrium concentration, transfer coefficient, chemical amount, Faraday constant, overpotential, gas constant, and temperature. Subscripts of O, R, a, and c respectively indicate oxidant, reductant, anode, and cathode. The reaction overpotential ΔV_{react} is related to the charge transfer process. If the mass transfer process is fast enough and the charge transfer process is a rate-determining process, the electrode surface concentration and equilibrium concentration of each reactant are regarded as being approximately equal ($C_R^s \approx C_R^{eq}$, $C_O^s \approx C_O^{eq}$). The current density of the reaction is therefore shown by the Butler−Volmer equation:

$$J = J_0 \cdot \left[\exp\left(\frac{\alpha_a n F \Delta V_{a\_react}}{RT} \right) - \exp\left(\frac{-\alpha_c n F \Delta V_{c\_react}}{RT} \right) \right] \quad (1)$$

Moreover, if the overpotential of each half reaction is high enough, the first or second term of Eqn (1) can be ignored and the remaining term simplifies to the Tafel equations:

$$\Delta V_{a\_react} = -\left(\frac{RT}{\alpha_a nF}\right)\cdot \ln J_{a\_0} + \left(\frac{RT}{\alpha_a nF}\right)\cdot \ln J_a$$

$$= -a_a + b_a \cdot \log J_a \qquad (2)$$

or

$$\Delta V_{c\_react} = \left(\frac{RT}{\alpha_c nF}\right)\cdot \ln J_{c\_0} - \left(\frac{RT}{\alpha_c nF}\right)\cdot \ln |J_c|$$

$$= a_c - b_c \cdot \log |J_c| \qquad (3)$$

a and b are respectively the intercept of Tafel equation and the Tafel slope. Each ΔV_{react} is calculated from the Tafel equations for anode and cathode reactions. Fig. S4 shows Tafel plots of the current density of H_2O oxidation or CO production at various potentials, and J_0 and the transfer coefficient α are calculated. Each ΔV_{react} is also estimated by the following equations:

$\Delta V_{a\_react} = 0.541 + 0.094 \cdot \log J_a$ (Ar bubbling)

$\Delta V_{a\_react} = 0.543 + 0.078 \cdot \log J_a$ (CO_2 bubbling)

$\Delta V_{c\_react} = 0.236 + 0.072 \cdot \log J_c$

In contrast, the concentration overpotential ΔV_{conc} is concerned with the mass transfer process. According to Fick's first law of diffusion, in the steady state the current density is expressed by the following equation:

$$J = nFS = nFD \cdot \frac{C^b - C^s}{\delta}$$

S, D, C^b, and δ are respectively the diffusion rate, diffusion coefficient, bulk concentration, and thickness of diffusion layer. If the overpotential of the half reaction is high enough and the mass transfer is a rate-determining step, the electrode surface concentration of reactant is regarded as zero ($C^s \approx 0$). Therefore, the maximum current density (limiting current density, $J_{\lim}$) is given by the following equations:

$$J_{a\_\lim} = nFD_R \cdot \frac{C_R^b}{\delta} \quad \text{or} \quad |J_{c\_\lim}| = nFD_O \cdot \frac{C_O^b}{\delta}$$

Moreover, if the bulk concentration and the equilibrium concentration are regarded as the same ($C^s \approx C^{eq}$), Eqn (1) can be written as the following equations:

$$\Delta V_a = -\left(\frac{RT}{\alpha_a nF}\right)\cdot \ln J_0 + \left(\frac{RT}{\alpha_a nF}\right)\cdot \ln J_a - \left(\frac{RT}{\alpha_a nF}\right)\cdot \ln\left(\frac{C_R^s}{C_R^b}\right)$$

or

$$\Delta V_c = \left(\frac{RT}{\alpha_c nF}\right)\cdot \ln J_0 - \left(\frac{RT}{\alpha_c nF}\right)\cdot \ln |J_c| + \left(\frac{RT}{\alpha_c nF}\right)\cdot \ln\left(\frac{C_O^s}{C_O^b}\right)$$

The first and second terms in the above equations exhibit ΔV_{react} (Eqn (2) and (3)), and the third term exhibits ΔV_{conc}.

$$\Delta V_{a\_conc} = -\left(\frac{RT}{\alpha_a nF}\right)\cdot \ln\left(\frac{C_R^s}{C_R^b}\right) \quad \text{or} \quad \Delta V_{c\_conc} = \left(\frac{RT}{\alpha_c nF}\right)\cdot \ln\left(\frac{C_O^s}{C_O^b}\right)$$

This equation is exhibited by J_{lim} as the following equations:

$$\Delta V_{a\_conc} = -\left(\frac{RT}{\alpha_a nF}\right)\cdot \ln\left(1-\frac{J_a}{J_{a\_\text{lim}}}\right)$$

or

$$\Delta V_{c\_conc} = \left(\frac{RT}{\alpha_c nF}\right)\cdot \ln\left(1-\frac{|J_c|}{|J_{c\_\text{lim}}|}\right)$$

Therefore, in Tafel plots (Fig. S4), the $\log(J_{\text{lim}})$ is exhibited by a convergence value at a potential far from the equilibrium potential.[1]

In addition, the resistance overpotential ΔV_{resist} is mainly generated from the resistance of the anion membrane, electrolytes, and electrodes. In this case the electrode resistance has little effect because the anode CoO_x layer is very thin and the cathode is composed of Au metal. ΔV_{resist} is therefore regarded as membrane and solution resistances, which is calculated by electrochemical impedance analysis.[2] Fig. S5 shows the Nyquist impedance spectra of the reaction cell at different electrolyte conditions. In the high frequency region, the reactance part is ignored and only the resistance part is observed. Therefore, the resistance at $-Z''_{\text{Im}} = 0$ is regarded as the membrane and solution resistances (ohmic resistance, R_{ohm}) and ΔV_{resist} is given by the following equation:

$$\Delta V_{reesist} = R_{ohm}\cdot J\cdot A$$

J and A are the operating current density and the electrode (acceptance) surface area, respectively. Therefore, the reaction activity of the electrodes is estimated by the following equation:

$$V = 1.33 + \Delta V_{react} + \Delta V_{conc} + \Delta V_{resist}$$
$$= 1.33 + \left(\frac{RT}{\alpha_a nF}\right)\cdot \ln\left(\frac{J}{J_0}\right) - \left(\frac{RT}{\alpha_c nF}\right)\cdot \ln\left(\frac{J}{J_0}\right)$$
$$-\left(\frac{RT}{\alpha_a nF}\right)\cdot \ln\left(1-\frac{J}{J_{a\_\text{lim}}}\right) + \left(\frac{RT}{\alpha_c nF}\right)\cdot \ln\left(1-\frac{J}{|J_{c\_\text{lim}}|}\right) + R_{ohm}\cdot J\cdot A$$

Moreover, when the pH is different between an anolyte and a catholyte, the liquid junction potential (ΔV_{pH}) is generated and acts as chemical bias. Therefore, the value of ΔV_{pH} must be deducted from V in the calculated equation. However, an accurate calculation of ΔV_{pH} is difficult, so we estimated ΔV_{pH} as the pH difference between anolyte and catholyte assuming that the major ion moving in the electrodes is hydroxide (OH^-). Therefore, the reaction activity is exhibited by the following equation:

$$
\begin{aligned}
V &= 1.33 + \Delta V_{react} + \Delta V_{conc} + \Delta V_{resist} - \Delta V_{pH} \\
&= 1.33 + \left(\frac{RT}{\alpha_a nF}\right)\cdot \ln\left(\frac{J}{J_0}\right) - \left(\frac{RT}{\alpha_c nF}\right)\cdot \ln\left(\frac{J}{J_0}\right) \\
&- \left(\frac{RT}{\alpha_a nF}\right)\cdot \ln\left(1 - \frac{J}{J_{a\_\lim}}\right) + \left(\frac{RT}{\alpha_c nF}\right)\cdot \ln\left(1 - \frac{J}{|J_{c\_\lim}|}\right) \\
&+ R_{ohm}\cdot J\cdot A - 0.0591\cdot \Delta\mathrm{pH}
\end{aligned}
\tag{4}
$$

Theoretical estimation of PV cell properties: In contrast, the PV cell property can be estimated from the current-voltage curve of the PV. In this simulation, the complicated 3jn-a-Si PV cell is regarded as a single-junction PV cell model for simplicity. The current-voltage curve of the PV cell is therefore exhibited by the following equation:[2]

$$
\begin{aligned}
J &= J_{ph} - J_d \\
&= J_{ph} - J_s\left\{\exp\left(\frac{q\left(V + J\cdot A\cdot R_s\right)}{n_i kT}\right) - 1\right\} - \frac{V + J\cdot A\cdot R_s}{R_{sh}\cdot A}
\end{aligned}
$$

J_{ph}, J_d, J_s, q, n_i, k, R_s, and R_{sh} are respectively the photocurrent density, dark current density, saturated current density, magnitude of the electrical charge on the electron, ideal factor of diode, Boltzmann constant, series sheet resistance, and shunt sheet resistance. However, the PV cell surface is coated with the CoO_x anode catalyst. The current-voltage curve therefore deceases due to its transmittance T_{sum}, which is estimated by integration as the follows equation:

$$
T_{sum} = \frac{\int_{300}^{850} T(\lambda) I(\lambda) d\lambda}{\int_{300}^{850} I(\lambda) d\lambda}
$$

$T(\lambda)$ and $I(\lambda)$ are respectively the transmittance of each wavelength and light intensity of each wavelength. The actual specific curve of the PV cell is thus given by the following equation.

$$
J = T_{sum} J_{ph} - J_s\left\{\exp\left(\frac{q\left(V + J\cdot A\cdot R_s\right)}{n_i kT}\right) - 1\right\} - \frac{V + J\cdot A\cdot R_s}{R_{sh}\cdot A}
\tag{5}
$$

The operating current density J is therefore the point of intersection between Eqn (4) and (5). Moreover, the partial current density of CO generation decreases the ratio of FE_{CO}. Therefore, the partial current density of CO generation J_{CO} is obtained by the following equation:

$$
J_{CO} = J\cdot FE_{CO}
$$

Theoretical estimation of faraday efficiency of CO FE_{CO}: The FE_{CO} in the reaction is estimated from the same results as the Tafel plots measurement. Fig. S6 shows the actual applied potentials of the Au nanoparticle cathode in the PV PEC system for CO production in the type A and B conditions (Fig. 3). The initial potentials for types A and B are −0.36 and −0.34 V vs. RHE, so the FE_{CO} is respectively estimated as 97% and 96% for types A and B.

Reference

1 J_{a_lim} at type B may be enough high than that at type A, and is regarded as the same value for type A.

2 K. Cui, A. S. Anisimov, T. Chiba, S. Fujii, H. Kataura, A. G. Nasibulin, S. Chiashi, E. I. Kauppinen, S. Maruyama, *J. Mater. Chem. A,* 2014, **2**, 11311-11318.

Table S1. Parameter values used to calculate the estimated solar-to-CO conversion efficiency.

Parameter		Type A	Type B
Gas constant	R [m^2 kg s^{-2} K^{-1} mol^{-1}]	8.315	
Temperature	T [K]	298.15	
Chemical amount	n [mol]	2	
Faraday constant	F [C mol^{-1}]	96500	
Elementary charge	q [C]	1.60×10^{-19}	
Ideal factor of diode	n_i [−]	1 ~ 2	
Boltzmann constant	k [m^2 kg s^{-2} K^{-1}]	1.38×10^{-23}	
Electrode (acceptance) surface area	A [m^2]	1.0	
PV cell			
Photocurrent density	J_{ph} [mA cm^{-2}]	5.51	
Saturated current density	J_0 [mA cm^{-2}]	480	
Series sheet resistance	R_s [Ω]	4.00	
Shunt sheet resistance	R_{sh} [Ω]	5.06×10^3	
Anode			
Tafel equation			
Tafel slope	b_a [V dec^{-1}]	0.094	0.078
Intercept of Tafel equation	a_a	−0.541	−0.543
Transfer coefficient	α_a	0.315	0.380
Exchange current density	J_{a_0} [mA cm^{-2}]	1.75×10^{-6}	1.06×10^{-7}
Limiting current density	J_{a_lim} [mA cm^{-2}]	15.1	15.1
Transmittance	T_{sum} [%]	69	
pH		9.2	7.3
Cathode			
Tafel equation			
Tafel slope	b_c [V dec^{-1}]	−0.056	
Intercept of Tafel equation	a_c	0.219	
Transfer coefficient	α_c	0.529	
Exchange current density	J_{c_0} [mA cm^{-2}]	5.31×10^{-4}	
Limiting current density	J_{c_lim} [mA cm^{-2}]	8.83	
Faraday efficiency of CO	FE_{CO} [%]	97	96
pH		7.3	
Ohmic resistance	R_{ohm} [Ω]	25.9	27.2
Estimated total current density	J_{-e} [mA cm^{-2}]	1.4	0.64
(experimental result at 10 min)	(J)	(1.6)	(0.92)
Estimated solar-to-CO conversion efficiency	$\eta_{CO\text{-}e}$ [%]	1.8	0.82
(experimental result at 10 min)	(η_{CO})	(2.3)	(1.28)

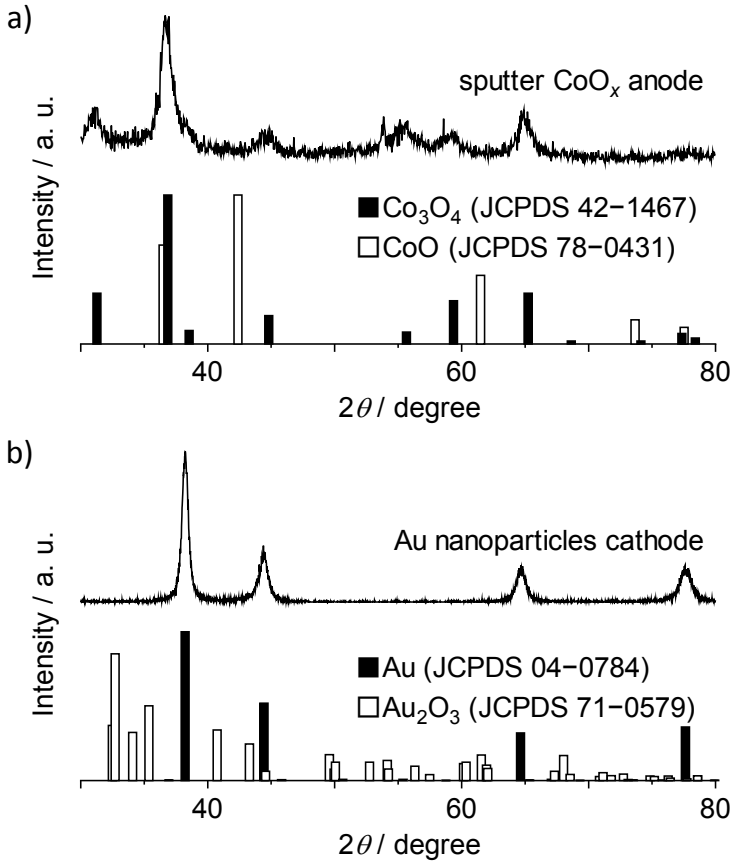

Fig. S1 XRD pattern of (a) CoO_x anode and (b) Au nanoparticle cathode.

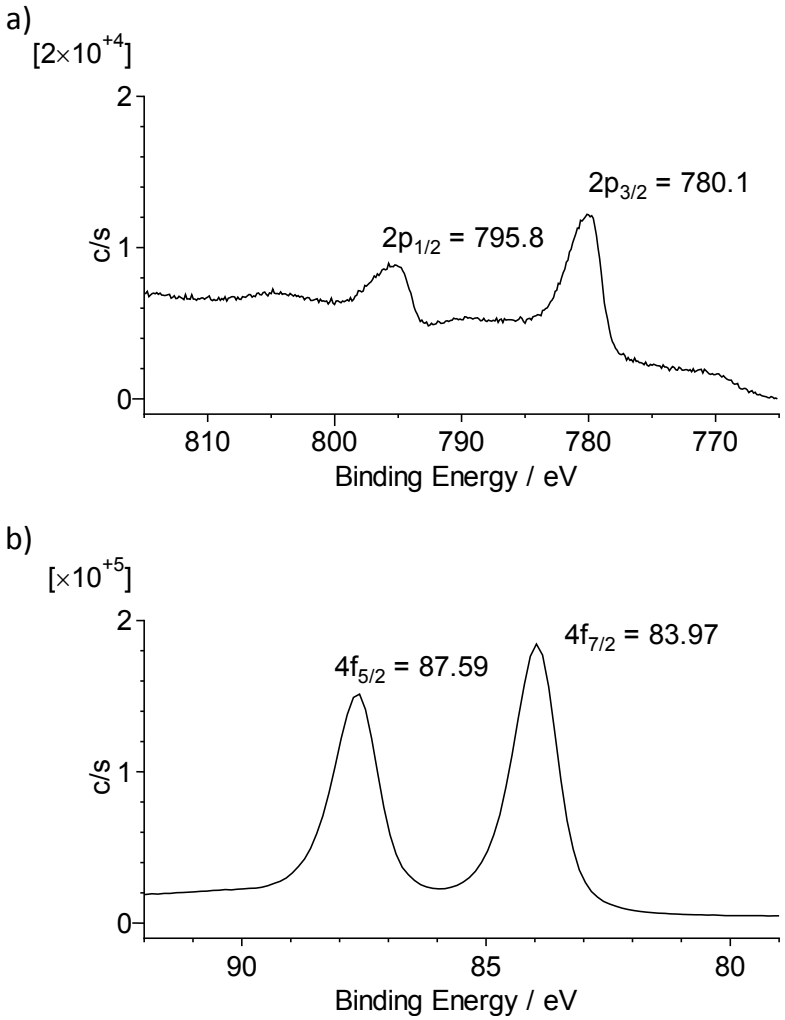

Fig. S2 XPS results for (a) CoO_x anode and (b) Au nanoparticle cathode.

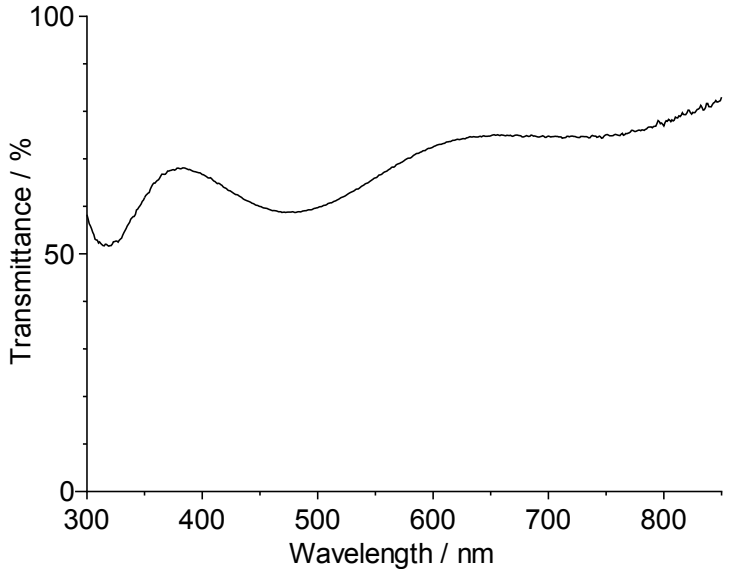

Fig. S3 Transmittance spectra of CoO_x anode on ITO/Si substrate.

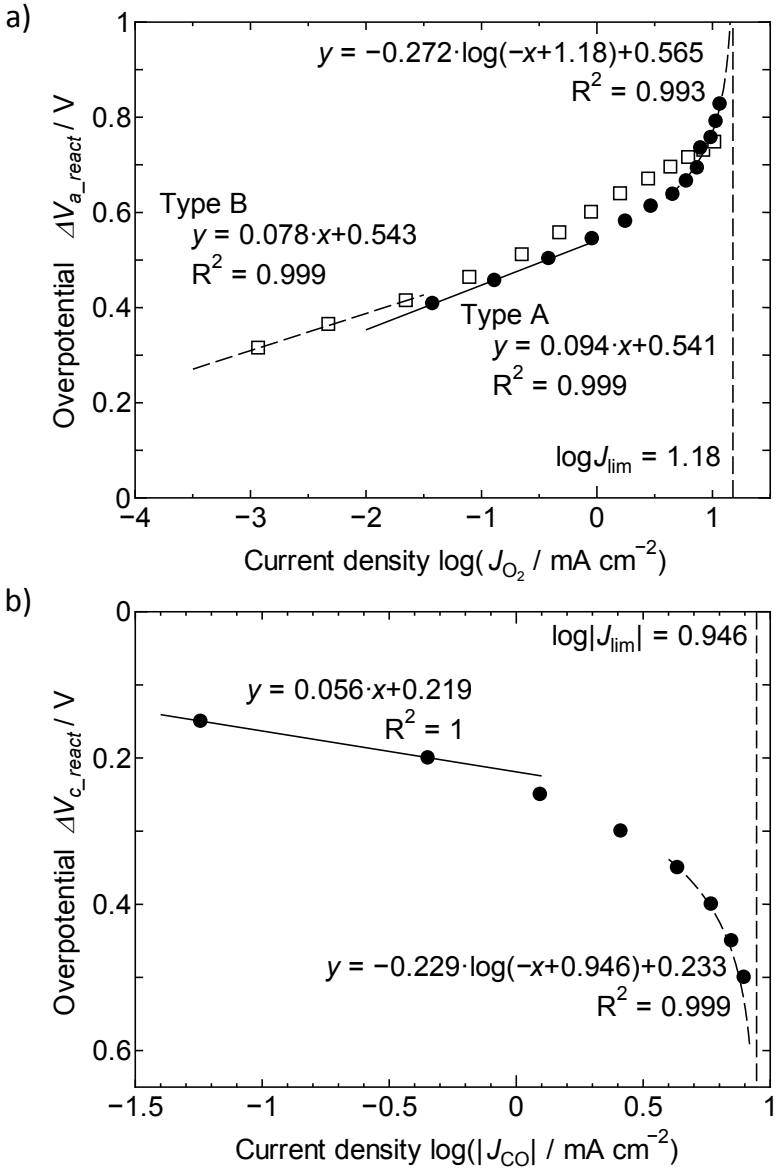

Fig. S4 Tafel plots of (a) anode electrode (●: type A and □: type B) and (b) cathode electrode.

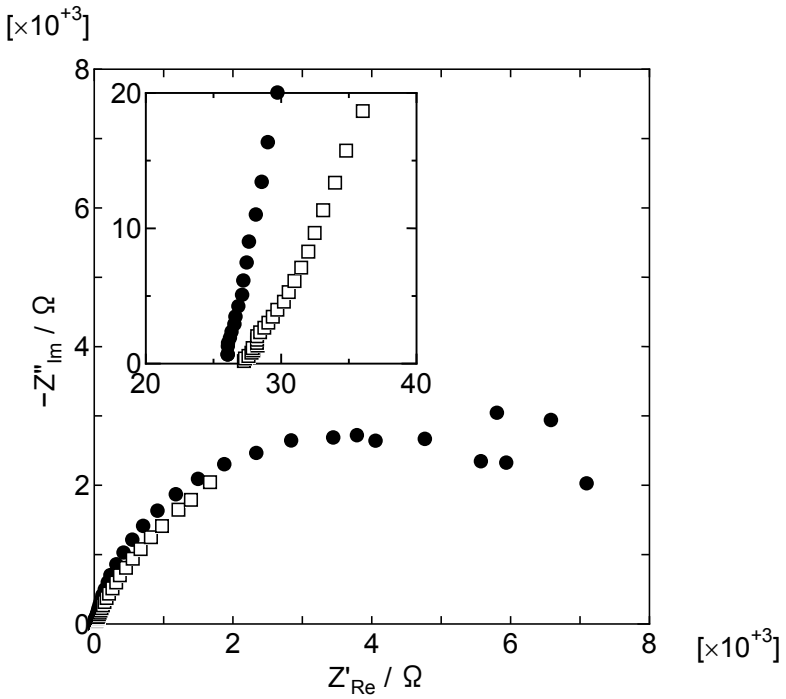

Fig. S5 Nyquist impedance spectra of the reaction cell at (●) the type A and (□) the type B.

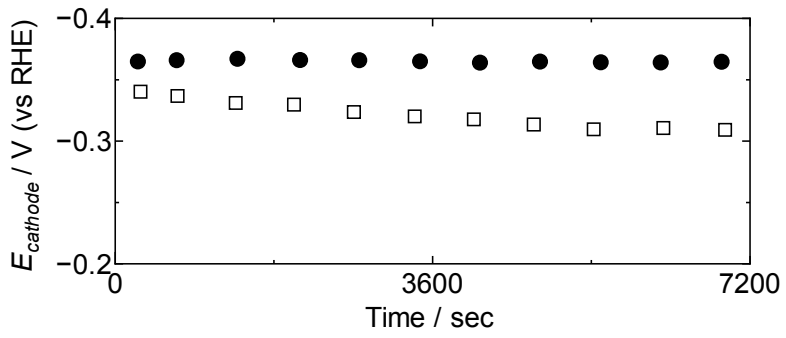

Fig. S6 Time-dependent changes in the applied potentials of Au nanoparticles cathode during the artificial photosynthesis of CO production at (●) type A and (□) type B. Reaction conditions are identical to those in Figure 2.